

# Study of $J/\psi$ decaying into $\omega p \bar{p}$

(BES Collaboration)

M. Ablikim<sup>1</sup>, J. Z. Bai<sup>1</sup>, Y. Ban<sup>11</sup>, X. Cai<sup>1</sup>, H. F. Chen<sup>16</sup>, H. S. Chen<sup>1</sup>, H. X. Chen<sup>1</sup>, J. C. Chen<sup>1</sup>, Jin Chen<sup>1</sup>, Y. B. Chen<sup>1</sup>, Y. P. Chu<sup>1</sup>, Y. S. Dai<sup>18</sup>, L. Y. Diao<sup>8</sup>, Z. Y. Deng<sup>1</sup>, Q. F. Dong<sup>14</sup>, S. X. Du<sup>1</sup>, J. Fang<sup>1</sup>, S. S. Fang<sup>1a</sup>, C. D. Fu<sup>14</sup>, C. S. Gao<sup>1</sup>, Y. N. Gao<sup>14</sup>, S. D. Gu<sup>1</sup>, Y. T. Gu<sup>4</sup>, Y. N. Guo<sup>1</sup>, Z. J. Guo<sup>15b</sup>, F. A. Harris<sup>15</sup>, K. L. He<sup>1</sup>, M. He<sup>12</sup>, Y. K. Heng<sup>1</sup>, J. Hou<sup>10</sup>, H. M. Hu<sup>1</sup>, J. H. Hu<sup>3</sup>, T. Hu<sup>1</sup>, G. S. Huang<sup>1c</sup>, X. T. Huang<sup>12</sup>, X. B. Ji<sup>1</sup>, X. S. Jiang<sup>1</sup>, X. Y. Jiang<sup>5</sup>, J. B. Jiao<sup>12</sup>, D. P. Jin<sup>1</sup>, S. Jin<sup>1</sup>, Y. F. Lai<sup>1</sup>, G. Li<sup>1</sup>, <sup>d</sup>, H. B. Li<sup>1</sup>, J. Li<sup>1</sup>, R. Y. Li<sup>1</sup>, S. M. Li<sup>1</sup>, W. D. Li<sup>1</sup>, W. G. Li<sup>1</sup>, X. L. Li<sup>1</sup>, X. N. Li<sup>1</sup>, X. Q. Li<sup>10</sup>, Y. F. Liang<sup>13</sup>, H. B. Liao<sup>1</sup>, B. J. Liu<sup>1</sup>, C. X. Liu<sup>1</sup>, F. Liu<sup>6</sup>, Fang Liu<sup>1</sup>, H. H. Liu<sup>1</sup>, H. M. Liu<sup>1</sup>, J. Liu<sup>11e</sup>, J. B. Liu<sup>1</sup>, J. P. Liu<sup>17</sup>, Jian Liu<sup>1</sup>, Q. Liu<sup>15</sup>, R. G. Liu<sup>1</sup>, Z. A. Liu<sup>1</sup>, Y. C. Lou<sup>5</sup>, F. Lu<sup>1</sup>, G. R. Lu<sup>5</sup>, J. G. Lu<sup>1</sup>, C. L. Luo<sup>9</sup>, F. C. Ma<sup>8</sup>, H. L. Ma<sup>2</sup>, L. L. Ma<sup>1f</sup>, Q. M. Ma<sup>1</sup>, Z. P. Mao<sup>1</sup>, X. H. Mo<sup>1</sup>, J. Nie<sup>1</sup>, S. L. Olsen<sup>15</sup>, R. G. Ping<sup>1</sup>, N. D. Qi<sup>1</sup>, H. Qin<sup>1</sup>, J. F. Qiu<sup>1</sup>, Z. Y. Ren<sup>1</sup>, G. Rong<sup>1</sup>, X. D. Ruan<sup>4</sup>, L. Y. Shan<sup>1</sup>, L. Shang<sup>1</sup>, C. P. Shen<sup>15</sup>, D. L. Shen<sup>1</sup>, X. Y. Shen<sup>1</sup>, H. Y. Sheng<sup>1</sup>, H. S. Sun<sup>1</sup>, S. S. Sun<sup>1</sup>, Y. Z. Sun<sup>1</sup>, Z. J. Sun<sup>1</sup>, X. Tang<sup>1</sup>, G. L. Tong<sup>1</sup>, G. S. Varner<sup>15</sup>, D. Y. Wang<sup>1g</sup>, L. Wang<sup>1</sup>, L. L. Wang<sup>1</sup>, L. S. Wang<sup>1</sup>, M. Wang<sup>1</sup>, P. Wang<sup>1</sup>, P. L. Wang<sup>1</sup>, W. F. Wang<sup>1h</sup>, Y. F. Wang<sup>1</sup>, Z. Wang<sup>1</sup>, Z. Y. Wang<sup>1</sup>, Zheng Wang<sup>1</sup>, C. L. Wei<sup>1</sup>, D. H. Wei<sup>1</sup>, Y. Weng<sup>1</sup>, N. Wu<sup>1</sup>, X. M. Xia<sup>1</sup>, X. X. Xie<sup>1</sup>, G. F. Xu<sup>1</sup>, X. P. Xu<sup>6</sup>, Y. Xu<sup>10</sup>, M. L. Yan<sup>16</sup>, H. X. Yang<sup>1</sup>, Y. X. Yang<sup>3</sup>, M. H. Ye<sup>2</sup>, Y. X. Ye<sup>16</sup>, G. W. Yu<sup>1</sup>, C. Z. Yuan<sup>1</sup>, Y. Yuan<sup>1</sup>, S. L. Zang<sup>1</sup>, Y. Zeng<sup>7</sup>, B. X. Zhang<sup>1</sup>, B. Y. Zhang<sup>1</sup>, C. C. Zhang<sup>1</sup>, D. H. Zhang<sup>1</sup>, H. Q. Zhang<sup>1</sup>, H. Y. Zhang<sup>1</sup>, J. W. Zhang<sup>1</sup>, J. Y. Zhang<sup>1</sup>, S. H. Zhang<sup>1</sup>, X. Y. Zhang<sup>12</sup>, Yiyun Zhang<sup>13</sup>, Z. X. Zhang<sup>11</sup>, Z. P. Zhang<sup>16</sup>, D. X. Zhao<sup>1</sup>, J. W. Zhao<sup>1</sup>, M. G. Zhao<sup>1</sup>, P. P. Zhao<sup>1</sup>, W. R. Zhao<sup>1</sup>, Z. G. Zhao<sup>11</sup>, H. Q. Zheng<sup>11</sup>, J. P. Zheng<sup>1</sup>, Z. P. Zheng<sup>1</sup>, L. Zhou<sup>1</sup>, K. J. Zhu<sup>1</sup>, Q. M. Zhu<sup>1</sup>, Y. C. Zhu<sup>1</sup>, Y. S. Zhu<sup>1</sup>, Z. A. Zhu<sup>1</sup>, B. A. Zhuang<sup>1</sup>, X. A. Zhuang<sup>1</sup>, and B. S. Zou<sup>1</sup>

- <sup>1</sup> Institute of High Energy Physics, Beijing 100049, People's Republic of China
- <sup>2</sup> China Center for Advanced Science and Technology (CCAST), Beijing 100080, People's Republic of China
- <sup>3</sup> Guangxi Normal University, Guilin 541004, People's Republic of China
- <sup>4</sup> Guangxi University, Nanning 530004, People's Republic of China
- <sup>5</sup> Henan Normal University, Xinxiang 453002, People's Republic of China
- <sup>6</sup> Huazhong Normal University, Wuhan 430079, People's Republic of China
- <sup>7</sup> Hunan University, Changsha 410082, People's Republic of China
- <sup>8</sup> Liaoning University, Shenyang 110036, People's Republic of China
- <sup>9</sup> Nanjing Normal University, Nanjing 210097, People's Republic of China
- <sup>10</sup> Nankai University, Tianjin 300071, People's Republic of China
- <sup>11</sup> Peking University, Beijing 100871, People's Republic of China
- <sup>12</sup> Shandong University, Jinan 250100, People's Republic of China
- <sup>13</sup> Sichuan University, Chengdu 610064, People's Republic of China
- <sup>14</sup> Tsinghua University, Beijing 100084, People's Republic of China
- <sup>15</sup> University of Hawaii, Honolulu, HI 96822, USA
- <sup>16</sup> University of Science and Technology of China, Hefei 230026, People's Republic of China
- <sup>17</sup> Wuhan University, Wuhan 430072, People's Republic of China
- <sup>18</sup> Zhejiang University, Hangzhou 310028, People's Republic of China

Received: date / Revised version: date

**Abstract.** The decay  $J/\psi \rightarrow \omega p \bar{p}$  is studied using a  $5.8 \times 10^7$   $J/\psi$  event sample accumulated with the BES II detector at the Beijing electron-positron collider. The decay branching fraction is measured to be  $B(J/\psi \rightarrow \omega p \bar{p}) = (9.8 \pm 0.3 \pm 1.4) \times 10^{-4}$ . No significant enhancement near the  $p \bar{p}$  mass threshold is observed, and an upper limit of  $B(J/\psi \rightarrow \omega X(1860))B(X(1860) \rightarrow p \bar{p}) < 1.5 \times 10^{-5}$  is determined at the 95% confidence level, where  $X(1860)$  designates the near-threshold enhancement seen in the  $p \bar{p}$  mass spectrum in  $J/\psi \rightarrow \gamma p \bar{p}$  decays.

<sup>a</sup> Current address: DESY, D-22607, Hamburg, Germany

<sup>b</sup> Current address: Johns Hopkins University, Baltimore, MD 21218, USA

<sup>c</sup> Current address: University of Oklahoma, Norman, OK 73019, USA

<sup>d</sup> Current address: Universite Paris XI, LAL-Bat. 208-BP34, 91898 ORSAY Cedex, France

## 1 Introduction

Decays of the  $J/\psi$  meson are regarded as being well suited for searches for new types of hadrons and for systematic studies of light hadron spectroscopy. Recently, a number of new structures have been observed in  $J/\psi$  decays. These include strong near-threshold mass enhancements in the  $p\bar{p}$  invariant mass spectrum from  $J/\psi \rightarrow \gamma p\bar{p}$  decays [1], the  $p\bar{\Lambda}$  and  $K^-\bar{\Lambda}$  threshold enhancements in the  $p\bar{\Lambda}$  and  $K^-\bar{\Lambda}$  mass spectra in  $J/\psi \rightarrow pK^-\bar{\Lambda}$  decays [2], the  $\omega\phi$  resonance in the  $\omega\phi$  mass spectrum in the double-OZI suppressed decay  $J/\psi \rightarrow \gamma\omega\phi$  [3], and a new resonance, the  $X(1835)$ , in  $J/\psi \rightarrow \gamma\pi^+\pi^-\eta'$  decays [4].

The enhancement  $X(1860)$  in  $J/\psi \rightarrow \gamma p\bar{p}$  can be fitted with an  $S$ - or  $P$ -wave Breit-Wigner (BW) resonance function. In the case of the  $S$ -wave fit, the mass is  $1859^{+3}_{-10} +^{+5}_{-25}$  MeV/ $c^2$  and the width is smaller than 30 MeV/ $c^2$  at the 90% confidence level (C.L.). It is of interest to note that a corresponding mass threshold enhancement is not observed in either  $p\bar{p}$  cross section measurements or in  $B$ -meson decays [5].

This surprising experimental observation has stimulated a number of theoretical interpretations. Some have suggested that it is a  $p\bar{p}$  bound state (*baryonium*) [6, 7, 8, 9, 10]. Others suggest that the enhancement is primarily due to final state interactions (FSI) between the proton and antiproton [11, 12].

The CLEO Collaboration published results on the radiative decay of the  $\Upsilon(1S)$  to the  $p\bar{p}$  system [13], where no  $p\bar{p}$  threshold enhancement is observed and the upper limit of the branching fraction is set at  $B(\Upsilon(1S) \rightarrow \gamma X(1860))B(X(1860) \rightarrow p\bar{p}) < 5 \times 10^{-7}$  at 90% C.L.. This enhancement is not observed in BES2  $\psi(2S) \rightarrow \gamma p\bar{p}$  data either [14] and the upper limit is set at  $B(\psi(2S) \rightarrow \gamma X(1860))B(X(1860) \rightarrow p\bar{p}) < 5.4 \times 10^{-6}$  at 90% C.L..

The investigation of the near-threshold  $p\bar{p}$  invariant mass spectrum in other  $J/\psi$  decay modes will be helpful in understanding the nature of the observed new structures and in clarifying the role of  $p\bar{p}$  FSI effects. If the enhancement seen in  $J/\psi \rightarrow \gamma p\bar{p}$  is from FSI, it should also be observed in other decays, such as  $J/\psi \rightarrow \omega p\bar{p}$ , which motivated our study of this channel. In this paper, we present results from an analysis of  $J/\psi \rightarrow \pi^+\pi^-\pi^0 p\bar{p}$  using a sample of  $5.8 \times 10^7 J/\psi$  decays recorded by the BESII detector at the Beijing Electron-Positron Collider (BEPC).

BES is a conventional solenoidal magnetic detector that is described in detail in Ref. [15]. BESII is the upgraded version of the BES detector [16]. A twelve-layer

Vertex Chamber (VC) surrounds a beryllium beam pipe and provides track and trigger information. A forty-layer main drift chamber (MDC) located just outside the VC provides measurements of charged particle trajectories over 85% of the total solid angle; it also provides ionization energy loss ( $dE/dx$ ) measurements that are used for particle identification (PID). A momentum resolution of  $\sigma_p/p = 1.78\%\sqrt{1+p^2}$  ( $p$  in GeV/ $c$ ) and a  $dE/dx$  resolution of  $\sim 8\%$  are obtained. An array of 48 scintillation counters surrounding the MDC measures the time of flight (TOF) of charged particles with a resolution of about 200 ps for hadrons. Outside of the TOF counters is a 12 radiation length, lead-gas barrel shower counter (BSC), that operates in self quenching streamer mode and measures the energies and positions of electrons and photons over 80% of the total solid angle with resolutions of  $\sigma_E/E = 0.21/\sqrt{E}$  ( $E$  in GeV/ $c^2$ ),  $\sigma_\phi = 7.9$  mrad, and  $\sigma_z = 2.3$  cm. External to a solenoidal coil, which provides a 0.4 T magnetic field over the tracking volume, is an iron flux return that is instrumented with three double-layer muon counters that identify muons with momentum greater than 500 MeV/ $c$ .

Monte-Carlo simulation is used to determine the mass resolution and detection efficiency, as well as to estimate the contributions from background processes. In this analysis, a GEANT3-based Monte-Carlo program (SIMBES), with a detailed simulation of the detector performance, is used. As described in detail in Ref. [17], the consistency between data and Monte-Carlo has been validated using many physics channels from both  $J/\psi$  and  $\psi(2S)$  decays.

## 2 Analysis of $J/\psi \rightarrow \omega p\bar{p}$ , $\omega \rightarrow \pi^+\pi^-\pi^0$

For candidate  $J/\psi \rightarrow \pi^+\pi^-\pi^0 p\bar{p}$  events, we require four well reconstructed charged tracks with net charge zero in the MDC and at least two isolated photons in the BSC. Each charged track is required to be well fitted to a helix, be within the polar angle region  $|\cos\theta| < 0.8$ , have a transverse momentum larger than 70 MeV/ $c$ , and have a point of closest approach of the track to the beam axis that is within 2 cm of the beam axis and within 20 cm from the center of the interaction region along the beam line. For each track, the TOF and  $dE/dx$  information is combined to form a particle identification confidence level for the  $\pi$ ,  $K$  and  $p$  hypotheses; the particle type with the highest confidence level is assigned to each track. The four charged tracks are required to consist of an unambiguously identified  $p$ ,  $\bar{p}$ ,  $\pi^+$  and  $\pi^-$  combination. An isolated neutral cluster is considered as a photon candidate when the angle between the nearest charged track and the cluster is greater than  $5^\circ$ , the angle between the  $\bar{p}$  track and the cluster is greater than  $25^\circ$  [18], the first hit is in the beginning of six radiation lengths of the BSC, the difference between the angle of the cluster development direction in the BSC and the photon emission direction is less than  $30^\circ$ , and the energy deposited in the shower counter is greater than 50 MeV. A four-constraint kinematic fit is performed to the hypothesis  $J/\psi \rightarrow p\bar{p}\pi^+\pi^-\gamma\gamma$ , and, in the cases where the number of photon candidates exceeds

<sup>e</sup> Current address: Max-Planck-Institut fuer Physik, Foehringer Ring 6, 80805 Munich, Germany

<sup>f</sup> Current address: University of Toronto, Toronto M5S 1A7, Canada

<sup>g</sup> Current address: CERN, CH-1211 Geneva 23, Switzerland

<sup>h</sup> Current address: Laboratoire de l'Accélérateur Linéaire, Orsay, F-91898, France

<sup>i</sup> Current address: University of Michigan, Ann Arbor, MI 48109, USA

Correspondence to: liubj@mail.ihep.ac.cn

two, the combination with the smallest  $\chi^2_{p\bar{p}\pi^+\pi^-\gamma\gamma}$  value is selected. We further require that  $\chi^2_{p\bar{p}\pi^+\pi^-\gamma\gamma} < 20$ .

Figure 1 shows the  $\gamma\gamma$  invariant mass of the events which survive the above-listed criteria, where a distinct  $\pi^0 \rightarrow \gamma\gamma$  signal is evident. Candidate  $\pi^0$  mesons are selected by requiring  $|M_{\gamma\gamma} - m_{\pi^0}| < 0.04 \text{ GeV}/c^2$ . After this selection, a total of 15260 events is retained. The  $\pi^+\pi^-\pi^0$  invariant mass spectrum for these events is shown as data points with error bars in Fig. 2, where prominent  $\omega$  and  $\eta$  signals are observed.

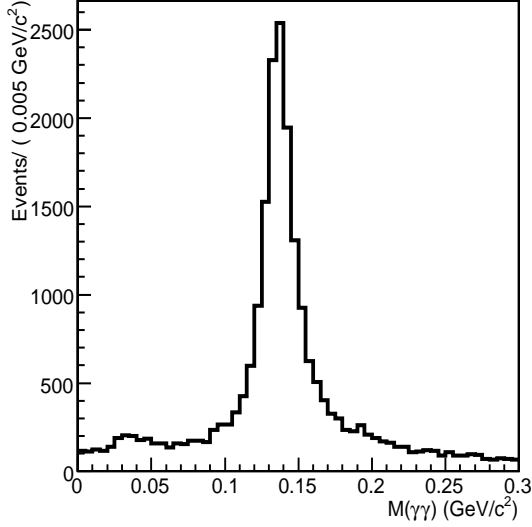


**Fig. 1.** The  $M_{\gamma\gamma}$  distribution for  $J/\psi \rightarrow \gamma\gamma\pi^+\pi^-\pi^0$  candidate events.

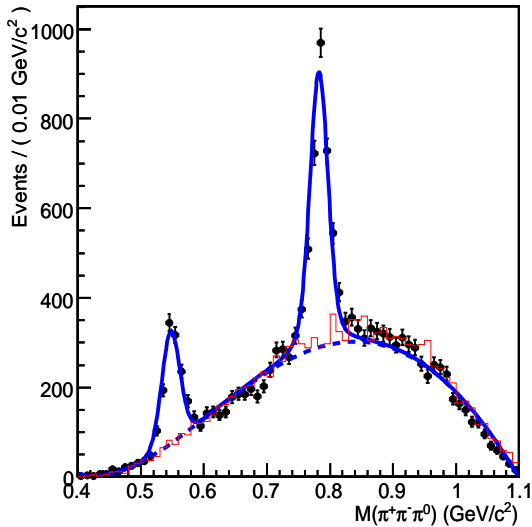


**Fig. 2.** The  $M_{\pi^+\pi^-\pi^0}$  distribution for  $J/\psi \rightarrow \pi^+\pi^-\pi^0 p\bar{p}$  candidate events. The dots with error bars are data. The solid histogram is the background estimated from Monte-Carlo simulation, normalized according to the PDG branching fractions. The solid curve is the result of a fit described in the text. The dashed curve is the background polynomial.

The backgrounds in the selected event sample are studied with Monte-Carlo simulations. We generated  $J/\psi \rightarrow p\bar{p}\pi^+\pi^-\pi^0$  decays as well as a variety of processes that are potential sources of background:  $J/\psi \rightarrow p\bar{p}\eta'(\eta' \rightarrow \pi^+\pi^-\eta)$ ;  $p\bar{p}\eta'(\eta' \rightarrow \rho^0\gamma)$ ;  $p\bar{p}\pi^+\pi^-$ ;  $\Lambda\bar{\Lambda}\pi^0$ ;  $\Sigma^0\bar{\Sigma}^0$ ;  $\Sigma(1385)^-\bar{\Sigma}^+$ ;  $\eta_c\gamma$ ;  $\Delta^{++}\Delta^{--}$ ;  $\gamma p\bar{p}\pi^+\pi^-$ ;  $\Delta^{++}\bar{p}\pi^-$ ;  $\Lambda\bar{\Sigma}^-\pi^+$  (+ c.c.);  $\Sigma^0\pi^0\bar{\Lambda}$ ;  $\Sigma(1385)^0\bar{\Sigma}^0$ ;  $\Delta^{++}\Delta^{--}\pi^0$ ; and  $\Xi^0\bar{\Xi}^0$ , in proportion to the branching fractions listed in the Particle Data Group (PDG) Tables [19]. The main background sources are found to be the decays  $J/\psi \rightarrow \Lambda\bar{\Sigma}^-\pi^+$  (+ c.c.) and  $\Delta^{++}\Delta^{--}\pi^0$ . The  $\pi^+\pi^-\pi^0$  invariant mass spectrum for background events that survive the selection criteria is shown as a solid histogram in Fig. 2; here no signal for  $\omega p\bar{p}$  is evident.

The branching fraction for  $J/\psi \rightarrow \omega p\bar{p}$  is computed using the relation

$$B(J/\psi \rightarrow \omega p\bar{p}) = \frac{N_{obs}}{N_{J/\psi} \cdot \varepsilon \cdot B(\omega \rightarrow \pi^+\pi^-\pi^0) \cdot B(\pi^0 \rightarrow \gamma\gamma)}.$$

Here,  $N_{obs}$  is the number of observed events;  $N_{J/\psi}$  is the number of  $J/\psi$  events,  $(57.7 \pm 2.6) \times 10^6$  [20];  $\varepsilon$  is the Monte-Carlo determined detection efficiency; and  $B(\omega \rightarrow \pi^+\pi^-\pi^0)$  and  $B(\pi^0 \rightarrow \gamma\gamma)$  are the  $\omega \rightarrow \pi^+\pi^-\pi^0$  and  $\pi^0 \rightarrow \gamma\gamma$  branching fractions.

The  $\pi^+\pi^-\pi^0$  invariant mass spectrum shown in Fig. 2 is fitted using an unbinned maximum likelihood fit with resolution broadened BW functions to represent the  $\omega$  and  $\eta$  signal peaks. The mass resolutions are obtained from Monte-Carlo simulation to be  $12 \text{ MeV}/c^2$  for the  $\omega$  and  $14 \text{ MeV}/c^2$  for the  $\eta$ . The masses and widths of the  $\omega$  and  $\eta$  are fixed at their PDG values [19]. A 4th-order Chebychev polynomial is used to describe the background. The fit gives an  $\omega$  signal yield of  $2449 \pm 69$  events. The detection efficiency from a uniform-phase-space Monte-Carlo simulation of  $J/\psi \rightarrow \omega p\bar{p}$  ( $\omega \rightarrow \pi^+\pi^-\pi^0$ ,  $\pi^0 \rightarrow \gamma\gamma$ ) is  $4.9 \pm 0.1\%$ . The branching fraction is determined to be:

$$B(J/\psi \rightarrow \omega p\bar{p}) = (9.8 \pm 0.3) \times 10^{-4},$$

where the error is statistical only.

We use this sample with  $|M_{\pi^+\pi^-\pi^0} - 0.783| < 0.03 \text{ GeV}/c^2$  to study the near-threshold region of the  $p\bar{p}$  invariant mass spectrum. Figure 3 shows a Dalitz plot for the selected  $J/\psi \rightarrow \omega p\bar{p}$  candidates, where no obvious structure is observed although it is not a uniform distribution. Figure 4 shows the threshold behavior of the  $p\bar{p}$  invariant mass distribution. The dotted curve in the figure indicates how the acceptance varies with invariant mass.

The backgrounds in the  $p\bar{p}$  threshold region mainly come from the decays of  $J/\psi \rightarrow \Lambda\bar{\Sigma}^-\pi^+$  (+ c.c.) and  $\Delta^{++}\Delta^{--}\pi^0$ . The  $M(p\bar{p})$  dependence of this background can be modeled by appropriately scaled data from the  $\omega$  sidebands ( $0.663 \text{ GeV}/c^2 < M_{\pi^+\pi^-\pi^0} < 0.723 \text{ GeV}/c^2$  and  $0.843 \text{ GeV}/c^2 < M_{\pi^+\pi^-\pi^0} < 0.903 \text{ GeV}/c^2$ ).

The contributions of sideband and non-resonant  $\omega p\bar{p}$  events can be well described by a function of the form

$$f(\delta) = N(\delta^{\frac{1}{2}} + a_1\delta^{\frac{3}{2}} + a_2\delta^{\frac{5}{2}})$$

with  $\delta \equiv M_{p\bar{p}} - 2m_p$ .

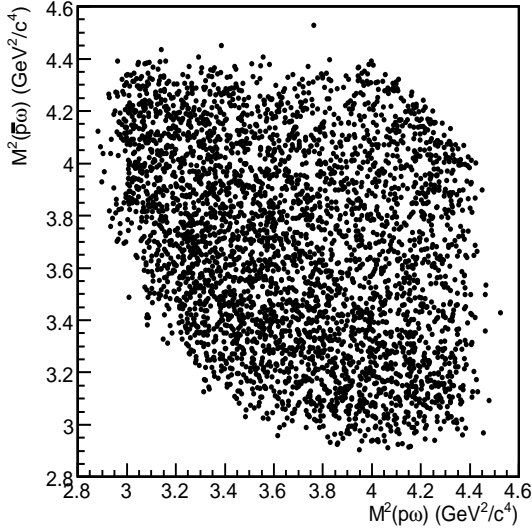


Fig. 3. The Dalitz plot for  $J/\psi \rightarrow \omega p\bar{p}$  candidate events.

In Fig. 4, no significant excess over the background plus non-resonant terms is evident. A Bayesian approach [19] is employed to extract the upper limit on the branching fraction of  $J/\psi \rightarrow \omega X(1860)$ . An acceptance-weighted  $S$ -wave BW function

$$BW(M) \propto \frac{q^{(2l+1)} k^3}{(M^2 - M_0^2)^2 + M_0^2 \Gamma^2} \cdot \varepsilon(M)$$

is used to represent the low-mass enhancement. Here,  $\Gamma$  is a constant width,  $q$  is the momentum of proton in the  $p\bar{p}$  rest frame,  $l$  is the relative orbital angular momentum of  $p$  and  $\bar{p}$ ,  $k$  is the momentum of  $\omega$ , and  $\varepsilon(M)$  is the detection efficiency obtained from Monte-Carlo simulation. The mass and width of the BW signal function are fixed to 1860 MeV/c<sup>2</sup> and 30 MeV/c<sup>2</sup>, respectively. The contributions of background and non-resonant  $\omega p\bar{p}$  events are presented by the function form  $f(\delta)$ , where the parameters  $a_1$  and  $a_2$  are allowed to float. As shown in Fig. 4, the solid curve is the fit of the  $M_{p\bar{p}} - 2m_p$  with the BW signal function and  $f(\delta)$  function described above. Using the Bayesian method, the 95% C.L. upper limit on the number of observed signal events is 29. Since the  $J^{PC}$  of  $X(1860)$  is unknown, we use simulated events distributed uniformly in phase space to determine a detection efficiency of  $J/\psi \rightarrow \omega X(1860)$  ( $X(1860) \rightarrow p\bar{p}$ ,  $\omega \rightarrow \pi^+\pi^-\pi^0$ ,  $\pi^0 \rightarrow \gamma\gamma$ ) of  $(4.7 \pm 0.1)\%$ . The upper limit of the branching fraction, without considering the systematic errors, is then:

$$\begin{aligned} & B(J/\psi \rightarrow \omega X(1860)) \cdot B(X(1860) \rightarrow p\bar{p}) \\ & < \frac{N_{obs}^{UL}}{N_{J/\psi} \cdot \varepsilon \cdot B(\omega \rightarrow \pi^+\pi^-\pi^0) \cdot B(\pi^0 \rightarrow \gamma\gamma)} = 1.2 \times 10^{-5}. \end{aligned}$$

### 3 Systematic errors

The systematic errors on the branching fractions are mainly due to uncertainties in the MDC tracking, kinematic fit-

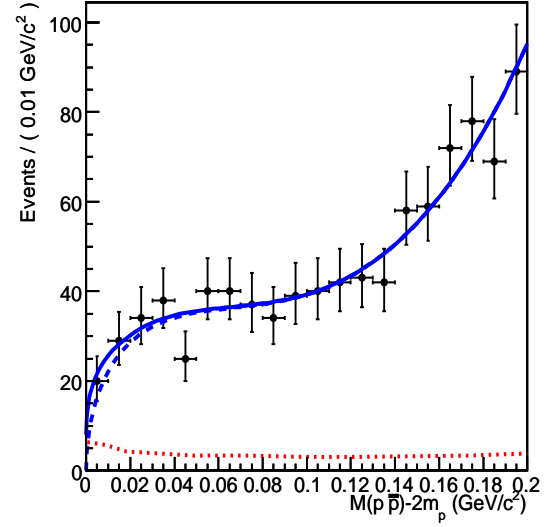


Fig. 4. The  $M_{p\bar{p}} - 2m_p$  distribution for  $J/\psi \rightarrow \omega p\bar{p}$  candidate events. The dots with error bars are data. The solid curve is the result of fit described in the text. The dashed curve is the function used to represent the background plus non-resonant  $\omega p\bar{p}$  events. The dotted curve indicates how the acceptance varies with  $p\bar{p}$  invariant mass.

ting, particle identification (PID), photon detection, background estimation, the model used to describe hadronic interactions in the material of the detector, and the uncertainty of the total number of  $J/\psi$  decays in the data sample.

The systematic error associated with the tracking efficiency has been carefully studied [17]. The difference of the tracking efficiencies between data and Monte-Carlo is 2% per charged track; an 8% contribution to the systematic error associated with the efficiency for detecting the four-track final state is assigned. In Ref. [17,21], the efficiencies for charged particle identification and photon detection are analyzed in detail. The systematic errors from PID and photon detection are 2% per proton (antiproton), 1% per pion and 2% per photon. In this analysis, with four charged tracks and two isolated photons; 6% is taken as the systematic error due to PID and 4% due to photon detection. The uncertainty due to kinematic fitting is studied using a number of exclusive  $J/\psi$  and  $\psi(2S)$  decay channels that are cleanly isolated without a kinematic fit [22,23]. It is found that the Monte-Carlo simulates the kinematic fit efficiency at the 5% or less level of uncertainty for almost all channels tested. Therefore, we take 5% as the systematic error due to the kinematic fit.

The background uncertainties come from the uncertainty of the background shape. For the branching fraction measurement of  $J/\psi \rightarrow \omega p\bar{p}$ , changing the order of the polynomial background causes an uncertainty in the number of background events. For the upper limit determination of  $J/\psi \rightarrow \omega X(1860)$ , the uncertainty of background shape can be determined by the fitting results with the background shape fixed to the function form  $f(\delta)$ , derived from fitting the scaled  $\omega$  sideband data plus phase-space generated  $\omega p\bar{p}$  MC events. Respectively, 5%

and 10% are taken as the systematic errors due to the background uncertainties in the branching fraction measurement of  $J/\psi \rightarrow \omega p\bar{p}$  and the upper limit determination of  $J/\psi \rightarrow \omega X(1860)$ .

Different simulation models for the hadronic interactions in the material of the detector (GALOR/FLUKA) [24, 25] give different efficiencies. Respectively, 4.8% and 11.4% are taken as the systemic errors due to the different hadronic models in the branching fraction measurement of  $J/\psi \rightarrow \omega p\bar{p}$  and the upper limit determination of  $J/\psi \rightarrow \omega X(1860)$ . In addition, if the  $J^P$  of  $X(1860)$  is  $0^-$ , the angular distribution of the  $\omega$  would be  $1 + \cos^2\theta$ . A Monte-Carlo sample generated with the  $\omega$  produced with a  $1 + \cos^2\theta$  distribution and a uniform distribution for the  $X(1860)$  decay into  $p\bar{p}$  results in an 8.5% reduction in detection efficiency. This difference is taken as the systematic error associated with the production model.

The branching fractions of  $\omega \rightarrow \pi^+\pi^-\pi^0$  and  $\pi^0 \rightarrow \gamma\gamma$  are taken from the PDG tables. The errors of the intermediate decay branching fractions, as well as the uncertainty of the number of  $J/\psi$  events [20] also result in the systematic errors in the measurements.

The systematic errors from the different sources are listed in Table 1. The total systematic errors for the branching fractions are obtained by adding up all the systematic sources in quadrature.

**Table 1.** Systematic error sources and contributions (%).

	B( $J/\psi \rightarrow \omega p\bar{p}$ )	Upper Limit
Tracking efficiency	8	8
Photon efficiency	4	4
Particle ID	6	6
Kinematic fit	5	5
Background uncertainty	5	10
Hadronic model	4.8	11.4
Production model	-	8.5
Intermediate decays	0.8	0.8
Total $J/\psi$ events	4.7	4.7
Total systematic error	14.6	21.6

## 4 Summary

With a  $5.8 \times 10^7 J/\psi$  event sample in the BESII detector, the branching fraction  $J/\psi \rightarrow \omega p\bar{p}$  is measured as:

$$B(J/\psi \rightarrow \omega p\bar{p}) = (9.8 \pm 0.3 \pm 1.4) \times 10^{-4}.$$

No obvious near-threshold  $p\bar{p}$  mass enhancement in  $J/\psi \rightarrow \omega p\bar{p}$  is observed, and the FSI interpretation of the  $p\bar{p}$  enhancement in  $J/\psi \rightarrow \gamma p\bar{p}$  is disfavored. A conservative estimate of the upper limit is determined by lowering the efficiency by one standard deviation. In this way, a 95% confidence level upper limit on the branching fraction

$$B(J/\psi \rightarrow \omega X(1860)) \cdot B(X(1860) \rightarrow p\bar{p}) < 1.5 \times 10^{-5}$$

is determined. The absence of the enhancement  $X(1860)$  in  $J/\psi \rightarrow \omega p\bar{p}$ ,  $\Upsilon(1S) \rightarrow \gamma p\bar{p}$  and  $\psi(2S) \rightarrow \gamma p\bar{p}$  also indicates its similar production property to that of  $\eta'$  [26, 27], *i.e.*,  $X(1860)$  is only largely produced in  $J/\psi$  radiative decays.

## 5 Acknowledgments

The BES collaboration thanks the staff of BEPC and computing center for their hard efforts. This work is supported in part by the National Natural Science Foundation of China under contracts Nos. 10491300, 10225524, 10225525, 10425523, 10625524, 10521003, the Chinese Academy of Sciences under contract No. KJ 95T-03, the 100 Talents Program of CAS under Contract Nos. U-11, U-24, U-25, and the Knowledge Innovation Project of CAS under Contract Nos. U-602, U-34 (IHEP), the National Natural Science Foundation of China under Contract No. 10225522 (Tsinghua University), and the Department of Energy under Contract No. DE-FG02-04ER41291 (U. Hawaii).

## References

1. J. Z. Bai *et al.* [BES Collaboration], Phys. Rev. Lett. **91**, 022001 (2003).
2. M. Ablikim *et al.* [BES Collaboration], Phys. Rev. Lett. **93**, 112002 (2004); H.X. Yang for the BES Collaboration, Int. J. Mod. Phys. **A20**, 1985 (2005).
3. M. Ablikim *et al.* [BES Collaboration], Phys. Rev. Lett. **96**, 162002 (2006).
4. M. Ablikim *et al.* [BES Collaboration], Phys. Rev. Lett. **95**, 262001 (2005).
5. S. Jin, invited plenary talk at ICHEP04, Beijing, 2004, Int. J. Mod. Phys. A **20**, 5145 (2005).
6. A. Datta and P. J. O'Donnell, Phys. Lett. B **567**, 273 (2003); M. L. Yan, S. Li, B. Wu and B. Q. Ma, Phys. Rev. D **72**, 034027 (2005); B. Loiseau and S. Wycech, Phys. Rev. C **72**, 011001 (2005).
7. J. R. Ellis, Y. Frishman and M. Karliner, Phys. Lett. B **566**, 201 (2003); J. L. Rosner, Phys. Rev. D **68**, 014004 (2003).
8. C. S. Gao and S. L. Zhu, Commun. Theor. Phys. **42**, 844 (2004).
9. G. J. Ding and M. L. Yan, Phys. Rev. C **72**, 015208 (2005).
10. I. S. Shapiro, Phys. Rept. **35**, 129 (1978); C. B. Dover and M. Goldhaber, Phys. Rev. D **15**, 1997 (1977).
11. B. S. Zou and H. C. Chiang, Phys. Rev. D **69**, 034004 (2004).
12. A. Sibirtsev, J. Haidenbauer, S. Krewald, U. G. Meissner and A. W. Thomas, Phys. Rev. D **71**, 054010 (2005).
13. S. B. Athar *et al.* [CLEO Collaboration], Phys. Rev. D **73**, 032001 (2006).
14. M. Ablikim *et al.* [BES Collaboration], Phys. Rev. Lett. **99**, 011802 (2007).
15. J. Z. Bai *et al.* [BES Collaboration], Nucl. Instrum. Meth. A **344**, 319 (1994).
16. J. Z. Bai *et al.* [BES Collaboration], Nucl. Instrum. Meth. A **458**, 627 (2001).
17. M. Ablikim *et al.* [BES Collaboration], Nucl. Instrum. Meth. A **552**, 344 (2005).

18. The annihilation of  $\bar{p}$  would produce many photons. Making the requestion of the angles between  $\bar{p}$  and photons more strict can effectively reduce the background from  $\bar{p}$  annihilation.
19. W. M. Yao *et al.* [Particle Data Group], J. Phys. G **33**, 1 (2006) and references therein.
20. The total number of  $J/\psi$  decays in the data sample is inferred from the total number of inclusive 4-prong hadronic decays; see FANG Shuangshi *et al.*, HEP&NP **27**, 277 (2003).
21. M. Ablikim *et al.* [BES Collaboration], Phys. Rev. Lett. **97**, 062001 (2006).
22. J. Z. Bai *et al.* [BES Collaboration], Phys. Rev. D **70**, 012005 (2004).
23. M. Ablikim *et al.* [BES Collaboration], Phys. Lett. B **610**, 192 (2005).
24. C. Zeitnitz and T. A. Gabriel, Nucl. Instrum. Meth. A **349**, 106 (1994).
25. K. Hanssger, H. J. Mohring and J. Ranft, Nucl. Sci. Eng. **88**, 551 (1984); J. Ranft and S. Ritter, Z. Phys. C **20**, 347 (1983); A Fasso *et al.*, FLUKA **92**, Proceedings of the Workshop on Simulating Accelerator Radiation Environment, Santa Fe (1993).
26. S. Jin for the BES Collaboration, talk at ICHEP06, Moscow, 2006
27. E. Klempt and A. Zaitsev, arXiv:0708.4016 [hep-ph].